MicroRNA-367-3p induces apoptosis and suppresses migration of MCF-7 cells by downregulating the expression of human choline kinase α

SWETA RAIKUNDALIA, SITI AISYAH FATEN MOHAMED SA'DOM, LING LING FEW and WEI CUN SEE TOO

School of Health Sciences, Health Campus, Universiti Sains Malaysia, Kubang Kerian, Kelantan 16150, Malaysia

Received June 10, 2020; Accepted November 16, 2020

DOI: 10.3892/ol.2021.12444

Abstract. Choline kinase (ChK) catalyzes the first step in the CDP-choline pathway for the synthesis of phosphatidylcholine. The α isoform of this enzyme is overexpressed in various types of cancer and its inhibition or downregulation has been applied as an anticancer strategy. In spite of increasing attention being paid to ChK expression, as well as its activity and inhibition in cancer, there are only limited studies available on the regulation of ChK, including its regulation by microRNAs (miRNAs/miRs). The dysregulation of gene expression by miRNAs is a common cause for carcinogenesis. In the present study, miR-367-3p was predicted to target the 3'-untranslated region (UTR) of the ChK α (*chka*) mRNA transcript. The binding of miR-367-3p to the 3'-UTR of *chka* was validated by a luciferase assay. The effects of the miR-367-3p mimic on *chka* gene and protein expression levels were determined by reverse transcription-quantitative polymerase chain reaction and western blot analysis, respectively. miR-367-3p significantly downregulated the expression of *chka* to ~60% of the negative control. Cells transfected with miR-367-3p exhibited higher levels of apoptosis and a lower cell migration compared with the control. To the best of our knowledge, the present study provided the first experimental evidence of the regulation of *chka* expression by miR-367-3p. The pro-apoptotic and suppressive effects of miR-367-3p on cell migration were similar to the anticancer effects resulting from the inhibition of ChK enzyme activity or the knockdown of *chka* gene expression by small interfering RNA. Therefore, these findings may potentially lead to the use of miR-367-3p in anticancer strategies that target ChK.

Correspondence to: Dr Wei Cun See Too or Dr Ling Ling Few, School of Health Sciences, Health Campus, Universiti Sains Malaysia, Kubang Kerian, Kelantan 16150, Malaysia
E-mail: stweicun@usm.my
E-mail: fewling@usm.my

Key words: choline kinase, microRNA, gene expression, cancer, apoptosis

Introduction

Choline kinase (ChK) catalyzes the phosphorylation of choline by using ATP as a phosphoryl donor. It is the first enzyme in the CDP-choline pathway for the *de novo* biosynthesis of phosphatidylcholine, the most abundant phospholipid in eukaryotic cell membrane (1). There are three isoforms of ChK in humans that are encoded by two separate genes known as *chka* and *chkb*. *chkb* codes for a single protein (ChKB), while *chka* undergoes alternative splicing to produce ChKA1 and ChKA2 isozymes (1). ChKA has been implicated in carcinogenesis, as this isoform is overexpressed in a variety of cancer types, including lung, breast, colon, ovarian and prostate cancer (2). By contrast, ChKB is crucial for muscle development, mitochondrial function and bone homeostasis (3).

ChKA serves an essential role in cell proliferation and transformation, as well as in the regulation of apoptosis and the cell cycle (4). The level of ChK and its product, phosphocholine are diagnostic indicators of cancer and markers for monitoring the tumor response to therapies (5). Due to the higher level of ChK expression in different cancer cells, the inhibition of ChKA activity has become a promising anticancer therapy. Consequently, the synthesis and testing of various ChKA inhibitors have gained increasing attention over the past decade (6). However, limited attention has been paid to the regulation of *chk* gene expression, particularly by microRNAs (miRNAs/miRs).

miRNAs are a large family of non-coding RNAs of ~21 nucleotides in length that regulate gene expression either by the degradation of target mRNAs or the inhibition of protein translation (7). miRNAs serve important roles in the immune system, differentiation, tumorigenesis and cell death (8). The dysregulation of miRNA expression is common in a number of types of cancer, and the miRNA profiling of clinical samples may be used for cancer diagnostic and prognostic applications (9). In humans, miR-195-5p functions as an anti-oncogene by targeting PHF-19, leading to the suppression of hepatoma cell invasion, migration and proliferation (10). Similarly, miR-7 has been demonstrated to exert an anti-metastatic effect on gastric cancer by targeting insulin-like growth factor-1 receptor (11). In certain cases, including the suppression of the Myc oncogenic pathway, the combined effects of several miRNAs have been observed (12). Therefore, a combined miRNA therapeutics approach to target lung cancer has been

proposed (13). In terms of drug discovery, the links between miRNAs and numerous human diseases and advances in anti-miR chemistries (chemical modifications for improved therapeutic properties) have suggested that the regulation of miRNAs may lead to the next revolution in pharmaceutical research (14). Until recently, there were ~20 clinical trials using miRNA- and small interfering RNA (siRNA)-based therapeutics (15). Strategies proposed for miRNA therapeutics include the artificial introduction of miRNAs or antisense oligonucleotides to inhibit miRNAs (16). In the present study, miR-367-3p was predicted and experimentally validated for the potential regulation of chka gene expression in breast cancer MCF-7 cells. The transfection of MCF-7 cells with miR-367-3p significantly downregulated *chka* expression, induced apoptosis and suppressed cell migration.

Materials and methods

Prediction of miRNAs targeting the human chka mRNA transcript. The prediction of miRNAs targeting the human *chka* mRNA transcript was performed using the microRNA.org website by submitting CHKA as the query gene symbol. The predicted miRNAs were ranked according to the mirSVR score (17). Minimum free energy (MFE) for miRNA binding to the target was predicted by RNAfold (18), mFold (19) and KineFold (20).

Cell lines, miRNA mimics, miRNA inhibitors, and chka-3'-untranslated region (UTR) firefly luciferase reporter plasmid. The malignant breast cancer MCF-7 (ATCC® HTB-22™) cell line, the cervical cancer HeLa (ATCC®CCL2™) cell line and the hepatoblastoma HepG2 (ATCC®HB8065™) cell line were obtained from the American Type Culture Collection and cultured in Dulbecco's modified Eagle's medium (DMEM; Gibco; cat. no. 41965039, Thermo Fisher Scientific, Inc.), containing 10% heat-inactivated fetal bovine serum (FBS; Gibco; cat. no. 26140087, Thermo Fisher Scientific, Inc.), 100 U/ml penicillin (cat. no. P0781, Sigma-Aldrich; Merck KGaA) and 100 mg/ml streptomycin (cat. no. 15140122, Sigma-Aldrich; Merck KGaA) in an incubator at 37˚C and 5% CO_2. The mimic for miR-367-3p (5'-AAUUGCACU UUAGCAAUGGUGA-3') and its inhibitor were purchased from Applied Biological Materials (cat. no. MCH01999). miRIDIAN microRNA mimic Housekeeping Positive Control #2 (GAPDH) (cat. no. CP-001000-02-05) and miRIDIAN microRNA mimic Negative Control #1 (cat. no. CN-001000-01-05) were purchased from GE Healthcare Dharmacon, Inc. The miRNA mimic was reconstituted in 1X siRNA buffer provided by the manufacturer. The firefly luciferase reporter construct containing the 3'-UTR of the *chka* gene (pMirTarget-*chka*-3'-UTR) was purchased from OriGene Technologies, Inc. (cat. no. SC212759).

Cell transfection. The miRNA mimics, inhibitors and plasmids were transiently transfected into adherent MCF-7 cells cultured in either 96-well (for miRNA target validation) or 24-well plates (for other experiments) using Lipofectamine® 3000 (cat. no. L3000015, Invitrogen; Thermo Fisher Scientific, Inc.). To begin with, $1x10^4$ and $1x10^5$ cells were seeded into 96-well and 24-well plates, respectively, and cultured for 16-18 h to achieve 70-80% confluency prior to transfection. The plasmid, miRNA mimic and miRNA inhibitor were diluted accordingly with Opti-MEM™ (cat. no. 31985062, Thermo Fisher Scientific, Inc.) to obtain final transfected concentrations of 200 ng pMirTarget-*chka*-3'UTR or pMirTarget empty vector, 25 nM miRNA mimic and 25 nM miRNA inhibitor. In another tube, Lipofectamine 3000 reagent (cat. no. L3000015, Invitrogen; Thermo Fisher Scientific, Inc.) was diluted with Opti-MEM™ according to the manufacturer's protocol. The two mixtures were mixed at a 1:1 ratio for 20 min at room temperature for the formation of transfection complexes. For target validation in the 96-well plate, 50 µl the transfection complexes were added to each well containing 50 µl fresh complete DMEM. The medium was replaced after 6 h and the cells were grown for a further 24 h prior to performing the firefly luciferase activity assay. For other experiments in the 24-well plate, 100 µl transfection complexes were added to each well containing 400 µl fresh complete DMEM, following by incubation for a further 48 h.

Firefly luciferase assay. After transfection with the pMirTarget-*chka*-3'-UTR plasmid containing the 3'-UTR of the *chka* gene together with mimic for miR-367-3p (5'-AAUUGCACU UUAGCAAUGGUGA-3') or microRNA Negative Control #1 (GE Healthcare Dharmacon, cat. no. CN-001000-01-05) and miR-367-3p inhibitor (Applied Biological Materials, cat. no. MCH01999) as described above, a total of 25 µl medium per well was removed from the 96-well plate and 75 µl the Dual-Glo luciferase reagent (cat. no. E2920, Promega Corporation) was added, followed by incubation at room temperature for 10 min. The firefly luciferase activity (relative light unit) was determined using the GloMax 20/20 luminometer (Promega Corporation). All luciferase assays were performed in triplicate and the experiment was repeated ≥2 times. The firefly luciferase activity of miRNA/inhibitor was normalized with that of miR-NC.

RNA isolation and reverse transcription-quantitative polymerase chain reaction (RT-qPCR). Total RNA was extracted from the MCF-7, HeLa or HepG2 cells transfected with miR-367-3p, miRIDIAN (negative control) or miR-GAPDH (positive control) using the Total RNA Isolation kit (cat. no. K0732, Thermo Fisher Scientific, Inc.) according to the manufacturer's protocol and genomic DNA removal was performed using the RNase-Free DNase set (cat. no. 79256, Qiagen GmbH). The RNA concentration was assessed using a Nano Drop ND-1000 spectrophotometer (Thermo Fisher Scientific, Inc.). Total RNA (1 µg) was reverse transcribed at 42˚C for 1 h using the RevertAid™ H minus First Strand cDNA Synthesis kit (cat. no. K1631, Thermo Fisher Scientific, Inc.) in a total volume of 20 µl. qPCR was performed using an ABI Prism 7500 Sequence Detection system (Thermo Fisher Scientific, Inc.) in a total reaction volume of 13 µl consisting of 6.25 µl Power SYBR™-Green PCR Master Mix (cat. no. 4367659, Thermo Fisher Scientific, Inc.), 0.5 µl each of forward and reverse primers, 1 µl cDNA and 4.75 µl double-distilled water. The PCR was run with an initial denaturation at 95˚C for 10 min, followed by 40 cycles of 95˚C (10 sec) and 60˚C (1 min);

chka 3′-UTR : 5′ GAAGCAGAAAUAUAGUGCAAUA 3′
miR-367-3p : 3′ AGUGGUAACGAUUUCACGUUAA 5′

Figure 1. Features of miR-367-3p and *chka* mRNA 3'-UTR pairing. The shaded sequence represents Watson-Crick base pairing at the seed region of miRNA. miR-367-3p binds the *chka* mRNA transcript (NM_001277.2) at nucleotides 1804-1825. miR, microRNA; *chka*, choline kinase α; UTR, untranslated region.

one cycle consisting of 95˚C for 15 sec, 60˚C for 1 min and 95˚C for 15 sec was introduced to obtain the dissociation curve for the analysis of PCR specificity. The primers used were as follows: Tyrosine 3-monooxygenase/tryptophan 5-monooxygenase activation protein ζ (YWHAZ) forward, 5'-TTCTTGATCCCCAATGCTTC-3' and reverse, 5'-ACT GGGTCTGGCCCTTAACT-3'; ribosomal protein S18 (RPS18) forward, 5'-TGTGGTGTTGAGGAAAGCA-3' and reverse, 5'-CTTCAGTCGCTCCAGGTCTT-3'; GAPDH forward, 5'-CAAGGTCATCCATGACAACTTTG-3' and reverse, 5'-GTCCACCACCCTGTTGCTGTAG-3'; and chka forward, 5'-TCAGAGCAAACATCCGGAAGT-3' and reverse, 5'-GGCGTAGTCCATGTACCCAAAT-3'. Relative gene expression levels normalized to the geometric mean of YWHAZ and RPS18 Cq values were determined using the $2^{-\Delta\Delta Cq}$ method (21).

Western blot analysis. Following 72 h of transfection, MCF-7 cell lysates were prepared using ProteoJET™ mammalian cell lysis reagent (Thermo Fisher Scientific, Inc.), according to the manufacturer's protocol. The protein concentration of the cell lysate was determined using Bradford assay reagent (cat. no. 5000006, Bio-Rad Laboratories, Inc.). Protein samples (30 μg) were loaded into the well of 12% SDS-PAGE. Following separation with 12% SDS-PAGE, the proteins were transferred onto a nitrocellulose membrane. The membrane was blocked with 5% (w/v) skimmed milk in TBST buffer for 1 h at room temperature prior to detection with rabbit primary β-actin (dilution, 1:5,000; cat. no. ab8227; Abcam) and Chka (dilution, 1:1,000; cat. no. ab88053; Abcam) antibodies overnight at 4˚C. The membrane was washed ≥3 times with TBST (0.1% (v/v) Tween-20 in TBS) buffer prior to incubation with HRP-conjugated secondary goat anti-rabbit IgG antibody (dilution, 1:5,000; cat. no. 12-348; Sigma-Aldrich, Merck KGaA) at room temperature for 1 h. The membrane was then washed three times prior to detection with SuperSignal™ West Femto maximum sensitivity substrate (cat. no. 34094, Thermo Fisher Scientific, Inc.). The signal was visualized using the FUSION FX chemiluminescence imaging system (Vilber Lourmat) and the band intensities were analyzed using ImageJ 1.49b software (National Institutes of Health).

Apoptotic and dead cell count. Cellular apoptosis was examined using the Muse™ Annexin V & Dead Cell Assay kit (cat. no. MCH100105, Merck Millipore) and analyzed using the Muse™ Cell Analyzer from EMD Millipore, according to the manufacturer's protocol. Transfected cells were detached by trypsinization, washed with PBS and resuspended in fresh DMEM (Gibco; Thermo Fisher Scientific, Inc.) containing

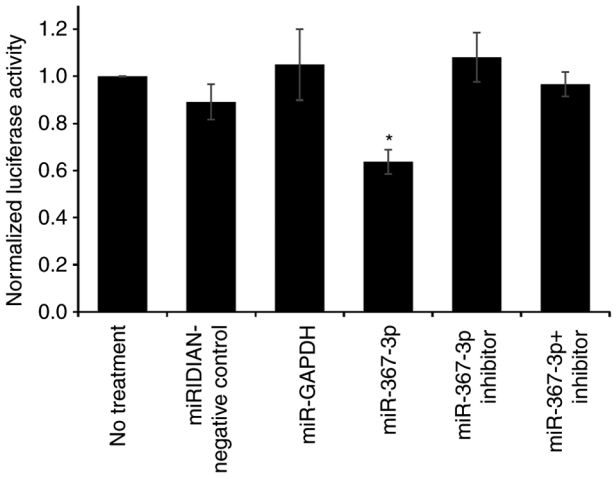

Figure 2. Target validation of miR-367-3p. MCF-7 cells transfected with the pMirTarget-*chka*-3'-UTR were treated individually or in combination with the specified miRNAs and miRNA inhibitors. Error bars indicate standard error of the mean from triplicate experiments. *P<0.05, compared with cells treated with the negative control miRNA. miR, microRNA; *chka*, choline kinase α; UTR, untranslated region.

10% FBS to at least $1x10^6$ cells/ml. In one tube, 100 μl cell suspension was mixed with 100 μl Muse™ Annexin V & Dead Cell reagent, vortexed using a benchtop vortex mixer and incubated for 30 min at room temperature in the dark. Stained cells were counted using a Muse™ Cell Analyzer, according to the manufacturer's protocol.

Scratch wound healing assay. Following treatment with miRNA mimics as described earlier, a diameter wide scratch wound was gently created using a P20 pipette tip into near confluent MCF-7 cells grown in a 6-well plate. The growth medium containing serum with detached cells after scratching was then discarded and the cells were washed twice before 2 ml fresh serum-free medium were added to each well. Images at the specified time points were captured using a DINO EYE eye-piece camera (AnMo Electronics Corporation) and the distance between the two edges of the scratch was measured using ImageJ 1.49b software (National Institutes of Health).

Statistical analysis. Data were analyzed using a Student's t-test or one-way analysis of variance followed by a Tukey's HSD *post hoc* test. P<0.05 was considered to indicate a statistically significant difference, and all analyses were performed using SPSS software version 22.0 (IBM Corp.). Data are presented as the mean ± standard error of mean from 3 independent experiments unless otherwise stated.

Results

miR-367-3p targets the 3'-UTR of chka mRNA. A total of 25 potential miRNAs targeting the 3'-UTR of the human *chka* mRNA transcript was predicted by microRNA.org. Hsa-miR-367-3p (miRBase accession no. MIMAT0000719) exhibited the highest mirSVR score of -1.0819. This miRNA targets the sequence from nucleotides 1804 to 1825 of the *chka* mRNA transcript (NM_001277.2). The analysis of MFE by

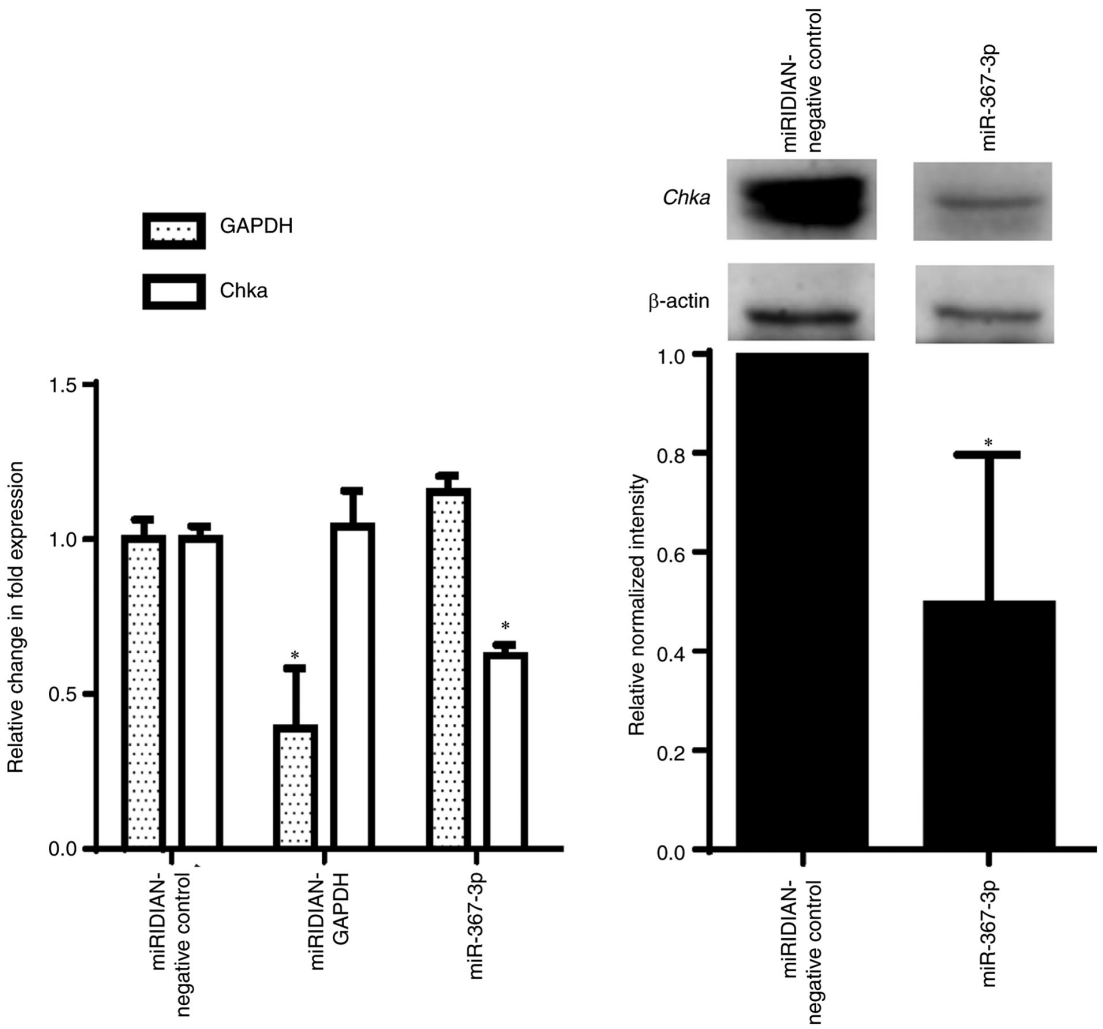

Figure 3. miR-367-3p downregulation of *chka* mRNA (left panel) and protein (right panel) expression. MCF-7 cells were transfected with 25 nM miR-367-3p mimic and *chka* mRNA and protein levels were determined by reverse transcription-quantitative polymerase chain reaction (at 48 h post-transfection) and western blot analysis (at 72 h post-transfection), respectively. Error bars indicate standard error of the mean from triplicate experiments. *P<0.05, compared with transfection with the miRIDIAN negative control. Western blots are representative results from triplicate experiments exhibiting a similar pattern. miR, microRNA; *chka*, choline kinase α.

RNAfold, mFold and KineFold predicted the strong binding of miR-367-3p to the target with MFE values of -3.1, -3.0 and -5.2 kcal/mol, respectively. As shown in Fig. 1, the base pairing at the seed region of miR-367-3p with the target sequence fell into the most favorable category known as 8-mer, which contains perfect Watson-Crick base pairing at position 2-8 of the miRNAs and an adenine nucleotide across from position 1 of the miRNAs (22).

Validation of the predicted miR-367-3p was performed using firefly luciferase and the 3'-UTR of the *chka* gene fusion construct (pMirTarget-*chka*-3'-UTR) in MCF-7 cells. As shown in Fig. 2, miR-367-3p significantly downregulated the relative firefly luciferase activity by ~40%, compared with the negative control miRNA-treated cells (P=0.033). Co-treatment with mir-367-3p inhibitor reversed the effect of its target miRNA, confirming the specific interaction between this miRNA and this target 3'-UTR. Treatment with the inhibitor alone slightly increased (not significant, P=0.9715) the relative firefly luciferase activity compared with the negative control, possibly due to the inhibition of endogenous miR-367-3p.

miR-367-3p downregulates the expression of chka in MCF-7, HeLa and HepG2 cell lines. The mimic of miR-367-3p was subsequently transfected into MCF-7 cells to assess the potential of this miRNA to downregulate the expression of the *chka* gene. As shown in Fig. 3 (left panel), miR-367-3p significantly downregulated *chka* expression to ~60%, compared with the negative control, which was similar to the level of downregulation observed in the aforementioned luciferase assay. Western blot analysis (Fig. 3, right panel) also revealed a significantly lower Chka protein expression of ~50%, compared with the negative control. The transfection of miR-367-3p into HeLa and HepG2 cell lines resulted in the significant suppression of *chka* mRNA levels (Fig. 4), as was observed in the MCF-7 cells. Taken together, these results confirmed the prediction that the *chka* mRNA transcript is targeted and downregulated by miR-367-3p.

miR-367-3p downregulation of chka expression induces cell death and suppresses cell migration. The inhibition of ChK activity and the knockdown of *chka* gene expression by RNA interference (RNAi) have been reported to induce cancer

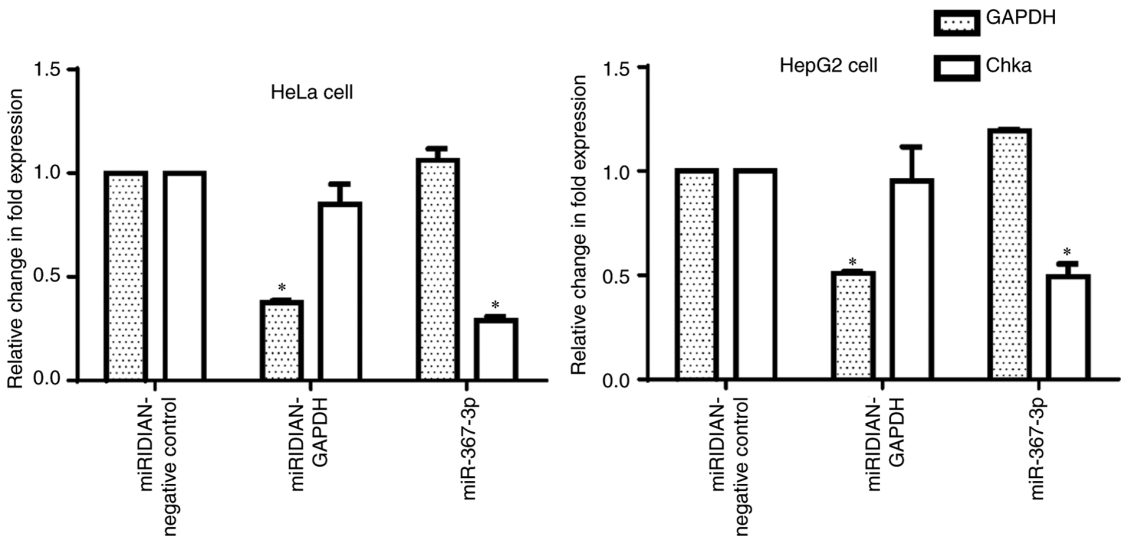

Figure 4. Downregulation of *chka* mRNA expression by miR-367-3p in the HeLa and HepG2 cell lines. Cells were transfected with 25 nM miR-367-3p mimic and the *chka* mRNA level was determined by reverse transcription-quantitative polymerase chain reaction at 48 h post-transfection. Error bars indicate the standard error of the mean from triplicate experiments. *P<0.05, compared with transfection with the miRIDIAN negative control. *chka*, choline kinase α; miR, microRNA.

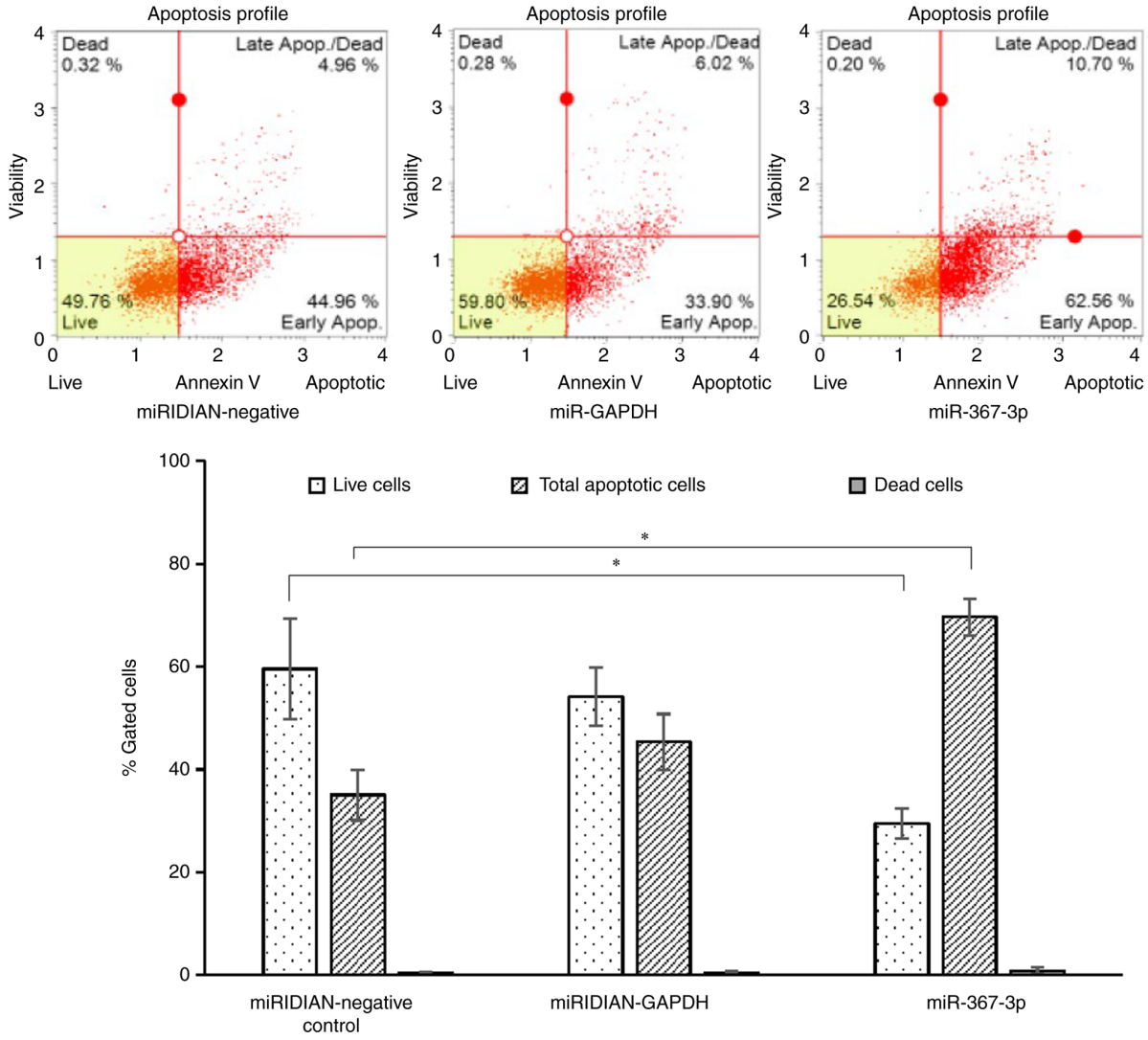

Figure 5. miR-367-3p induces a higher level of MCF-7 cell apoptosis. Cells were transfected with 25 nM each miRNA mimic for 48 h, stained with Muse™ Annexin V and Dead Cell reagent and counted with a Muse™ Cell analyzer. *P<0.05, compared with transfection with the miRIDIAN negative control. miR, microRNA; *chka*, choline kinase α.

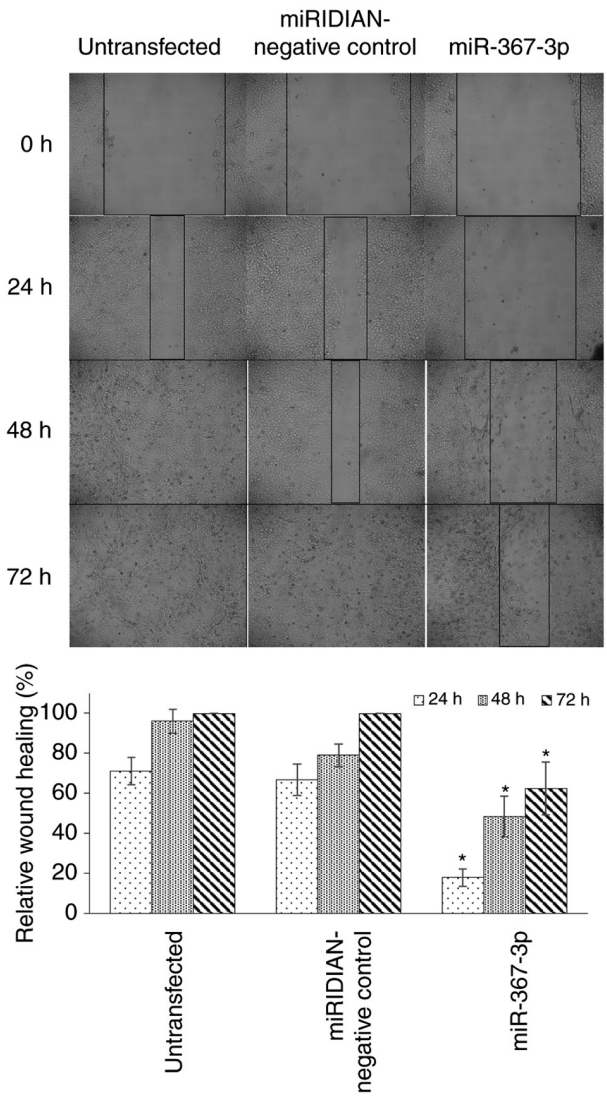

Figure 6. miR-367-3p suppresses MCF-7 cell migration. Cells were transfected with 25 nM miR-367-3p mimic for 48 h and representative images of wound healing at 0, 24, 48 and 72 h are shown in the upper panel. The box indicates the area where the wound gap was measured at 3 different locations. Images are representatives from triplicate experiments with similar results. The relative percentage of wound healing is depicted in the lower panel. *P<0.05 at the respective time points with untransfected cells and cells transfected with negative control miRNA. miR, microRNA.

cell death (4). Therefore, the effect of miR-367-3p mimic on cellular apoptosis was investigated in the present study. Based on the results presented in Fig. 5, statistically significant differences were observed in the percentages of live cells and total apoptotic cells between the cells transfected with negative control miRNA and the miR-367-3p-transfected cells. These results suggested that miR-367-3p induced cell death by targeting *chka*. The inhibition of ChKa activity has been demonstrated to decrease the migration of tumor cells (23,24). Therefore, the present study investigated whether the downregulation of *chka* expression by miR-367-3p was able to suppress MCF-7 cell migration. As shown in Fig. 6, miR-367-3p treatment significantly suppressed cell migration, with only ~60% closure of the scratch, compared with complete closure in the untreated and negative control cells after 72 h.

Discussion

ChK overexpression has been implicated in various types of cancer. The inhibition of the activity and the downregulation of the expression of this enzyme have been applied as promising anticancer strategies (6). However, the mechanisms that lead to the higher expression of ChK in cancer cells are not yet well understood. The present study investigated the possibility of the regulation of *chka* gene expression by miRNAs. miR-367-3p was predicted to target the 3'-UTR of the *chka* mRNA transcript with strong affinity, based on low values of mirSVR and MFEs. Target prediction analysis is crucial as the subsequent experimental validation of miRNAs is time-consuming and costly (25). mirSVR offers the optimal performance among other prediction tools when the ranking of the output is required (25). MFE of a miRNA-target interaction is one of the determinants of the silencing efficiency, as indicated by the improved silencing of the *Arabidopsis MYB81* gene by miR-159 following mutation to incorporate the sequence for improved binding by miR-159 (26).

miR-367-3p originates from the 3'-end of the hairpin loop sequence of miR-367, which is expressed as the miR-302/367 cluster. This cluster of miRNAs is mainly expressed in embryonic stem cells and is able to reprogram somatic cells into pluripotency (27). miR-367-3p has been reported to enhance the efficacy of Sorafenib chemotherapy to suppress hepatocellular carcinoma metastasis by enhancing the pathway involving the androgen receptor (28). However, the ectopic expression of miR-367-3p in non-small cell lung cancer cells has been demonstrated to promote cell proliferation and cell cycle progression, and inhibit apoptosis (29). According to Yan *et al* (30), the same miRNA may serve different roles in different types of cancer cell by acting as either an oncogene or tumor suppressor. The contradictory effects of miR-367 (whether this was miR-367-3p or miR-367-5p was not specified) on cancer cell growth and the response to drugs have been reported (31-35). The overexpression of miR-367 in paclitaxel-sensitive ovarian cancer cells has been demonstrated to further enhance the sensitivity to this drug (31). The overexpression of miR-367 has also been demonstrated to inhibit the migration and invasion of gastric cancer (32). By contrast, a higher expression of miR-367 has been found to be associated with an unfavorable prognosis of high-grade glioma (33), resected non-small cell lung cancer (34) and pancreatic ductal adenocarcinoma (35). Therefore, the effects of miR-367-3p on cancer cell survival may be cell type-dependent. The results of the present study suggested that this miRNA may be used as a novel therapeutic agent against breast cancer cells overexpressing ChK. The suppression of Runx2 by miR-135 and miR-203 has been shown to inhibit breast cancer cell migration *in vitro*, as well as tumor growth and metastasis *in vivo* (36). The results of wound healing assay in the present study also demonstrated that the suppression of *chka* by miR-367-3p inhibited MCF-7 breast cancer cell migration *in vitro*, which may produce the same anti-metastatic effect *in vivo*.

Due to the higher level of *chka* expression in different cancer cells, the inhibition of Chka activity has become a promising anticancer therapy. Consequently, the synthesis and testing of various small-molecule Chka inhibitors have gained increasing attention over the past decade (6). The inhibition of Chka enzyme activity

or the knockdown of *chka* gene expression by RNAi specifically induces the death of cancer cells, but not that of normal cells (1). The RNAi of *chka* has been demonstrated to decrease tumor cell viability and enhance the efficacy of prodrug enzyme activation treatment in cancer therapy (37). Recently, degradable dextran nanopolymer, which is less toxic and more suitable for cancer therapy, has been synthesized to deliver siRNA targeting *chka* in breast cancer cells (38). mir-367-3p, which downregulates the *chka* gene, as reported in the present study, may also be used in a similar manner. Replenishing tumor suppressor miRNAs, including miR-34 by lipid nanoparticles, miR-200 by liposomal carriers and miR-26a by the adeno-associated virus-mediated expression is one the approaches in miRNA therapeutics (39). The downregulation of the *chka* gene by RNAi or miRNAs may be more effective than activity inhibition by small molecules alone in killing cancer cells, based on the ChKA non-catalytic role in promoting cancer cell survival (40).

The anti-proliferative effects of miRNAs have previously been reported in humans. For example, miR-195-5p functions as an anti-oncogene by targeting PHF-19, leading to the suppression of hepatoma cell invasion, migration and proliferation (10). Similarly, miR-7 has been shown to exert an anti-metastatic effect on gastric cancer by targeting insulin-like growth factor-1 receptor (11). In the present study, it was confirmed that the 3'-UTR of the *chka* transcript was the target of miR-367-3p and the expression of *chka* was downregulated by this miRNA. The decreased level of *chka* resulted in higher levels of apoptosis and a lower migration of MCF-7 cells. Although the expression of miR-367-3p was not determined following the transfection of its mimic or inhibitor, the downregulation of the target (*chka*) gene expression by the miR-367-3p mimic was consistent throughout all the experiments in the present study. The results of the present study suggested that miR-367-3p may be a promising miRNA candidate for further investigation into the roles of miRNAs in cancer development involving the dysregulation of *chka* gene expression. However, further studies are required to elucidate the effects of *chka* downregulation by miR-367-3p on cell proliferation, invasion and anticancer drug resistance in more cancer cell lines in order to fully understand the role of *chka* attenuation by this miRNA in cancer.

Acknowledgements

Not applicable.

Funding

The present study was supported by the Universiti Sains Malaysia Individual Research University Grant (grant no. 1001/PPSK/8012239) and the Malaysia Ministry of Higher Education Fundamental Research Grant Scheme (grant no. 203/PPSK/6171222), and Ms Raikundalia was a PhD candidate supported by the Malaysia International Scholarship.

Availability of data and materials

The data generated and/or analyzed during the present study are available from the corresponding author upon reasonable request.

Authors' contributions

SR and SAFMS performed the experiments and analyzed the data. LLF designed the experiments, analyzed the data and drafted the initial manuscript. WCST conceived and designed the experiments, analyzed the data and was a major contributor in drafting the manuscript. All authors have read and approved the final manuscript.

Ethics approval and consent to participate

Not applicable.

Patient consent for publication

Not applicable.

Competing interests

The authors declare that they have no competing interests.

References

1. Arlauckas SP, Popov AV and Delikatny EJ: Choline kinase alpha-putting the choK-hold on tumor metabolism. Prog Lipid Res 63: 28-40, 2016.
2. Sanchez-Lopez E, Zimmerman T, Gomez del Pulgar T, Moyer MP, Lacal Sanjuan JC and Cebrian A: Choline kinase inhibition induces exacerbated endoplasmic reticulum stress and triggers apoptosis via CHOP in cancer cells. Cell Death Dis 4: e933, 2013.
3. Chang CC, Few LL, Konrad M and See Too WC: Phosphorylation of human choline kinase beta by protein kinase A: Its impact on activity and inhibition. PLoS One 11: e0154702, 2016.
4. Gruber J, See Too WC, Wong MT, Lavie A, McSorley T and Konrad M: Balance of human choline kinase isoforms is critical for cell cycle regulation: Implications for the development of choline kinase-targeted cancer therapy. FEBS J 279: 1915-1928, 2012.
5. Wu G and Vance DE: Choline kinase and its function. Biochem Cell Biol 88: 559-564, 2010.
6. Gómez-Pérez V, McSorley T, See Too WC, Konrad M and Campos JM: Novel 4-amino bis-pyridinium and bis-quinolinium derivatives as choline kinase inhibitors with antiproliferative activity against the human breast cancer SKBR-3 cell line. ChemMedChem 7: 663-669, 2012.
7. Gebert LFR and MacRae IJ: Regulation of microRNA function in animals. Nat Rev Mol Cell Biol 20: 21-37, 2019.
8. Hirschberger S, Hinske LC and Kreth S: miRNAs: Dynamic regulators of immune cell functions in inflammation and cancer. Cancer Lett 431: 11-21, 2018.
9. Lan H, Lu H, Wang X and Jin H: MicroRNAs as potential biomarkers in cancer: Opportunities and challenges. Biomed Res Int 2015: 125094, 2015.
10. Xu H, Hu YW, Zhao JY, Hu XM, Li SF, Wang YC, Gao JJ, Sha YH, Kang CM, Lin L, *et al*: MicroRNA-195-5p acts as an anti-oncogene by targeting PHF19 in hepatocellular carcinoma. Oncol Rep 34: 175-182, 2015.
11. Zhao X, Dou W, He L, Liang S, Tie J, Liu C, Li T, Lu Y, Mo P, Shi Y, *et al*: MicroRNA-7 functions as an anti-metastatic microRNA in gastric cancer by targeting insulin-like growth factor-1 receptor. Oncogene 32: 1363-1372, 2013.
12. Bueno MJ, Gómez de Cedrón M, Gómez-López G, Pérez de Castro I, Di Lisio L, Montes-Moreno S, Martínez N, Guerrero M, Sánchez-Martínez R, Santos J, *et al*: Combinatorial effects of microRNAs to suppress the Myc oncogenic pathway. Blood 117: 6255-6266, 2011.
13. Kasinski AL, Kelnar K, Stahlhut C, Orellana E, Zhao J, Shimer E, Dysart S, Chen X, Bader AG and Slack FJ: A combinatorial microRNA therapeutics approach to suppressing non-small cell lung cancer. Oncogene 34: 3547-3555, 2015.
14. van Rooij E, Purcell AL and Levin AA: Developing microRNA therapeutics. Circ Res 110: 496-507, 2012.

15. Chakraborty C, Sharma AR, Sharma G, George C, Doss CGP and Lee SS: Therapeutic miRNA and siRNA: Moving from bench to clinic as next generation medicine. Mol Ther Nucleic Acid 8: 132-143, 2017.
16. Broderick JA and Zamore PD: MicroRNA therapeutics. Gene Ther 18: 1104-1110, 2011.
17. Betel D, Koppal A, Agius P, Sander C and Leslie C: Comprehensive modeling of microRNA targets predicts functional non-conserved and non-canonical sites. Genome Biol 11: R90, 2010.
18. Lorenz WA and Clote P: Computing the partition function for kinetically trapped RNA secondary structures. PLoS One 6: e16178, 2011.
19. Zuker M: Mfold web server for nucleic acid folding and hybridization prediction. Nucleic Acids Res 31: 3406-3415, 2003.
20. Xayaphoummine A, Bucher T and Isambert H: Kinefold web server for RNA/DNA folding path and structure prediction including pseudoknots and knots. Nucleic Acids Res 33 (Web Server Issue): W605-W610, 2005.
21. Livak KJ and Schmittgen TD: Analysis of relative gene expression data using real-time quantitative PCR and the 2(-Delta Delta C(T)) method. Methods 25: 402-408, 2001.
22. Friedman RC, Farh KK, Burge CB and Bartel DP: Most mammalian mRNAs are conserved targets of microRNAs. Genome Res 19: 92-105, 2009.
23. Granata A, Nicoletti R, Tinaglia V, De Cecco L, Pisanu ME, Ricci A, Podo F, Canevari S, Iorio E, Bagnoli M and Mezzanzanica D: Choline kinase-alpha by regulating cell aggressiveness and drug sensitivity is a potential druggable target for ovarian cancer. Br J Cancer 110: 330-340, 2014.
24. Mariotto E, Viola G, Ronca R, Persano L, Aveic S, Bhujwalla ZM, Mori N, Accordi B, Serafin V, López-Cara LC and Bortolozzi R: Choline kinase alpha inhibition by EB-3D triggers cellular senescence, reduces tumor growth and metastatic dissemination in breast cancer. Cancers (Basel) 10: 391, 2018.
25. Oliveira AC, Bovolenta LA, Nachtigall PG, Herkenhoff ME, Lemke N and Pinhal D: Combining results from distinct MicroRNA target prediction tools enhances the performance of analyses. Front Genet 8: 59, 2017.
26. Zheng Z, Reichel M, Deveson I, Wong G, Li J and Millar AA: Target RNA secondary structure is a major determinant of miR159 efficacy. Plant Physiol 174: 1764-1778, 2017.
27. Rosa A and Brivanlou AH: Regulatory non-coding RNAs in pluripotent stem cells. Int J Mol Sci 14: 14346-14373, 2013.
28. Xu J, Lin H, Li G, Sun Y, Chen J, Shi L, Cai X and Chang C: The miR-367-3p increases sorafenib chemotherapy efficacy to suppress hepatocellular carcinoma metastasis through altering the androgen receptor signals. EBioMedicine 12: 55-67, 2016.
29. Xiao G, Gao X, Sun X, Yang C, Zhang B, Sun R, Huang G, Li X, Liu J, Du N, *et al*: miR-367 promotes tumor growth by inhibiting FBXW7 in NSCLC. Oncol Rep 38: 1190-1198, 2017.
30. Yan W, Jiang X, Wang G, Li W, Zhai C, Chen S, Shang F, Zhao Z and Yu W: Cyto-biological effects of microRNA-424-5p on human colorectal cancer cells. Oncol Lett 20: 120, 2020.
31. Chen N, Chon HS, Xiong Y, Marchion DC, Judson PL, Hakam A, Gonzalez-Bosquet J, Permuth-Wey J, Wenham RM, Apte SM, *et al*: Human cancer cell line microRNAs associated with in vitro sensitivity to paclitaxel. Oncol Rep 31: 376-383, 2014.
32. Bin Z, Dedong H, Xiangjie F, Hongwei X and Qinghui Y: The microRNA-367 inhibits the invasion and metastasis of gastric cancer by directly repressing Rab23. Genet Test Mol Biomarkers 19: 69-74, 2015.
33. Guan Y, Chen L, Bao Y, Qiu B, Pang C, Cui R and Wang Y: High miR-196a and low miR-367 cooperatively correlate with unfavorable prognosis of high-grade glioma. Int J Clin Exp Pathol 8: 6576-6588, 2015.
34. Campayo M, Navarro A, Vinõlas N, Diaz T, Tejero R, Gimferrer JM, Molins L, Cabanas ML, Ramirez J, Monzo M and Marrades R: Low miR-145 and high miR-367 are associated with unfavourable prognosis in resected nonsmall cell lung cancer. Eur Respir J 41: 1172-1178, 2013.
35. Zhu Z, Xu Y, Zhao J, Liu Q, Feng W, Fan J and Wang P: miR-367 promotes epithelial-to-mesenchymal transition and invasion of pancreatic ductal adenocarcinoma cells by targeting the Smad7-TGF-β signalling pathway. Br J Cancer 112: 1367-1375, 2015.
36. Taipaleenmäki H, Browne G, Akech J, Zustin J, van Wijnen AJ, Stein JL, Hesse E, Stein GS and Lian JB: Targeting of Runx2 by miR-135 and miR-203 impairs progression of breast cancer and metastatic bone disease. Cancer Res 75: 1433-1444, 2015.
37. Li C, Penet MF, Wildes F, Takagi T, Chen Z, Winnard PT, Artemov D and Bhujwalla ZM: Nanoplex delivery of siRNA and prodrug enzyme for multimodality image-guided molecular pathway targeted cancer therapy. ACS Nano 4: 6707-6716, 2010.
38. Chen Z, Krishnamachary B and Bhujwalla ZM: Degradable dextran nanopolymer as a carrier for choline kinase (Chok) siRNA cancer therapy. Nanomaterials (Basel) 6: 34, 2016.
39. Rupaimoole R and Slack FJ: MicroRNA therapeutics: Towards a new era for the management of cancer and other diseases. Nat Rev Drug Discov 16: 203-222, 2017.
40. Falcon SC, Hudson CS, Huang Y, Mortimore M, Golec JM, Charlton PA, Weber P and Sundaram H: A non-catalytic role of choline kinase alpha is important in promoting cancer cell survival. Oncogenesis 2: e38, 2013.